ASLO Limnology and Oceanography: Methods

Sedimentation Event Sensor: new ocean instrument for in-situ imaging and fluorometry of sinking particulate matter

Journal:	*Limnology and Oceanography: Methods*
Manuscript ID	LOM-16-04-0056
Wiley - Manuscript type:	New Methods
Date Submitted by the Author:	14-Apr-2016
Complete List of Authors:	McGill, Paul; Monterey Bay Aquarium Research Institute Henthorn, Richard; MBARI, Research Bird, Larry; MBARI, Research Huffard , Christine ; Monterey Bay Aquarium Research Institute, Pelagic Benthic Coupling Klimov, Dennis; Monterey Bay Aquarium Research Institute Smith, Ken; Monterey Bay Aquarium Research Institute, Pelagic Benthic Coupling
Keywords:	autonomous oceanographic instrumentation, macrophotography, sediment trap, sinking particulate matter
Abstract:	Measuring the quantity and composition of sinking particulate matter is key to understanding biogeochemical processes in the ocean. This has been done in the past with sequencing sediment traps, which collect and store particulate matter in sample bottles for subsequent laboratory analysis. Having a limited number of bottles, these traditional traps force the user to choose between finer time resolution and longer deployment duration. We have built a new sediment trap that analyzes the collected material in situ, eliminating the need to preserve and store the samples. This new instrument, the Sedimentation Event Sensor (SES), captures macro images of the sample with front and back lighting, and takes fluorometric measurements in two bands as proxies for the presence of chlorophyll a and accessory pigments. The SES can process 5,600 samples during a single deployment, which is the equivalent of 15 samples per day for more than a year. Here we describe the design of the SES and present the results of its first three deployments at 3910 m depth.

Sedimentation Event Sensor: new ocean instrument for in-situ imaging and fluorometry of sinking particulate matter

Paul R. McGill[1*], Richard G. Henthorn[1], Larry E. Bird[1], Christine L. Huffard[1], Dennis V. Klimov[1], and Kenneth L. Smith, Jr. [1]

[1]Monterey Bay Aquarium Research Institute

*Corresponding author: Monterey Bay Aquarium Research Institute, 7700 Sandholdt Rd, Moss Landing, CA 95039; Phone: +1-831-775-1738; email: mcgill@mbari.org

Running head— Sedimentation Event Sensor

Keywords— autonomous oceanographic instrumentation, macrophotography, sediment trap, sinking particulate matter

Abstract

Measuring the quantity and composition of sinking particulate matter is key to understanding biogeochemical processes in the ocean. This has been done in the past with sequencing sediment traps, which collect and store particulate matter in sample bottles for subsequent laboratory analysis. Having a limited number of bottles, these traditional traps force the user to choose between finer time resolution and longer deployment duration. We have built a new sediment trap that analyzes the collected material in situ, eliminating the need to preserve and store the samples. This new instrument, the Sedimentation Event Sensor (SES), captures macro images of the sample with front and back lighting, and takes fluorometric measurements in two bands as proxies for the presence of chlorophyll *a* and accessory pigments. The SES can process 5,600 samples during a single deployment, which is the equivalent of 15 samples per day for more than a year. Here we describe the design of the SES and present the results of its first three deployments at 3910 m depth.

Introduction

Resolving biogeochemical cycling in the ocean is heavily dependent on measuring particulate matter fluxes. Funnels and cylinders have been used over the past four decades to collect particulate matter sinking through the water column and to estimate fluxes of biogenic and mineral material in all major regions of the world ocean (Knauer et al. 1979; Honjo 1980). These sediment traps can be either moored at discrete depths through the water column or on autonomous free-drifting devices set to float at pre-determined depths or density surfaces (Buesseler et al. 2007). To estimate particle fluxes all of these designs require the retrieval and subsequent laboratory analysis of collected samples, which are typically chemically preserved in situ. Sequencing sediment traps, which open and close a series of collection bottles at pre-programmed times, are typically necessary for producing long time-series collections, but are limited by the number of sample bottles available (Honjo and Doherty 1988).

Our goal was to develop an instrument, the Sedimentation Event Sensor (SES), that could 1) be moored at abyssal depths, 2) temporarily capture particulate matter sinking through the water column, 3) produce high-resolution images of collected particulates, 4) make fluorometric measurements to estimate the chlorophyll content of collected particulates, 5) work at any desired sampling frequency from hours to days, for deployment periods of up to a year, and 6) discard the particulates collected rather than preserving samples for subsequent laboratory analysis. The resulting time-series of high-definition images and optical data could then be processed to estimate biological origin, quantity, size distribution, and fluorescent quality of sinking particulate matter without the need to store or preserve samples, or handle toxic preservatives. For biogenic material, the organic carbon and nitrogen

content could then be estimated from similar material collected concurrently in conventional sediment traps.

Here we describe the design of the SES, developed at the Monterey Bay Aquarium Research Institute, and assess mechanical performance and scientific lessons learned from early testing and its first three deployments spanning 21 months.

Materials and procedure

Overview

The SES is a stand-alone, self-powered instrument built into an open titanium frame, deployable at depths up to 4000 m. A large plastic funnel collects sinking particulate matter and channels it onto a movable sample plate. After the programmed sample period, the sample plate is positioned under a fluorometer to detect fluorescence consistent with the presence of chlorophyll *a* and accessory pigments, and then under a digital camera to record both front- and back-lit images. Finally, the sample is discarded and the sample plate is cleaned by brushes before the empty plate is positioned back under the funnel to collect the next sample.

Mechanical hardware

The core of the SES mechanical design is a commercially available sediment trap (McLane Laboratories model Mark78H-21). The polyethylene sample funnel is 80 cm in diameter with a collection area of 0.5 m^2. The titanium frame (Fig. 1) was modified to function as the bottom-most element in a vertical mooring string, although the instrument can be deployed at any position along a vertical mooring line. A 165 kg steel drop weight on a wire rope holds the SES 50 m above the seafloor, while a series of five 0.11 m^3 syntactic foam floats provide buoyancy above the SES. Mounts were added to the frame to accommodate two deep-sea acoustic releases (Teledyne Benthos model 865-A). An auxiliary

frame extension, 92 cm in diameter and 78 cm in length, was added to the base of the Parflux frame to accommodate a titanium pressure sphere and drop-weight release mechanism. The titanium pressure sphere contains the necessary electronics and batteries to power the system, and the tandem acoustic release mechanism provides redundancy to drop the ballast weight, allowing the instrument to ascend to the surface for recovery. The instrument weighs 147 kg in water, is 2.61 m in height and 0.92 m in diameter.

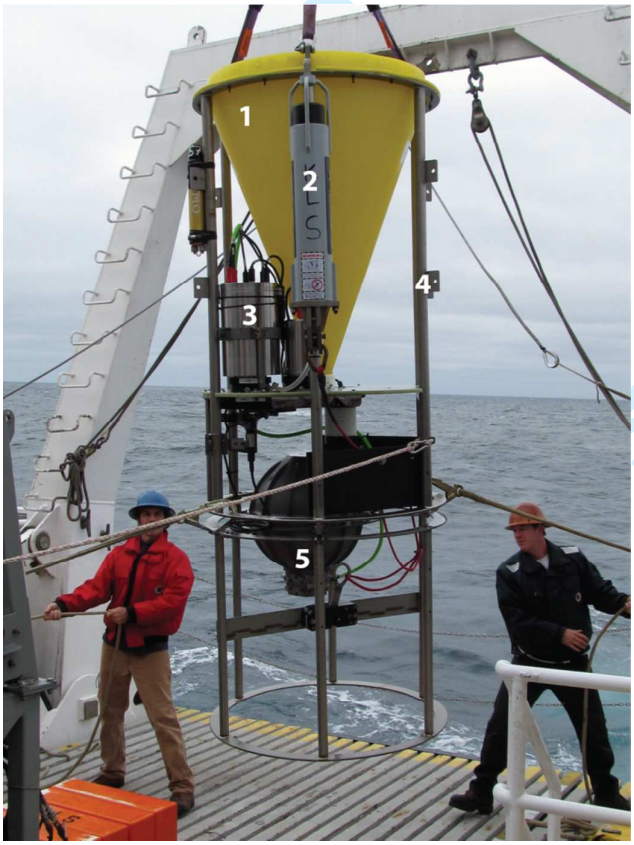

Figure 1. The SES being prepared for deployment. The instrument is deployed as part of a 140-m-long mooring string. Components shown: 1) funnel, 2) acoustic release, 3) camera and controller housing, 4) titanium frame, 5) battery sphere.

Figure 2 shows the relative placement of the SES system components. The existing sample bottle carousel was replaced with a new sample assembly (Fig. 3). This assembly

allows the horizontal sample plate, mounted beneath the funnel during the collection period, to rotate into position beneath the fluorometer or camera for analysis or imaging. As the rotation continues, a cam-driven mechanism moves the sample plate to a vertical orientation, dumping the sample. The plate then passes between a pair of cleaning brushes to remove any accumulated material before starting the next collection cycle. At the completion of one revolution the sample plate is back in position below the funnel, ready for the next sample collection. The camera and fluorometer housings are mounted near the base of the collection funnel vertically, with their viewports looking down. The battery sphere is centered inside the frame at the bottom of the instrument (Fig. 2).

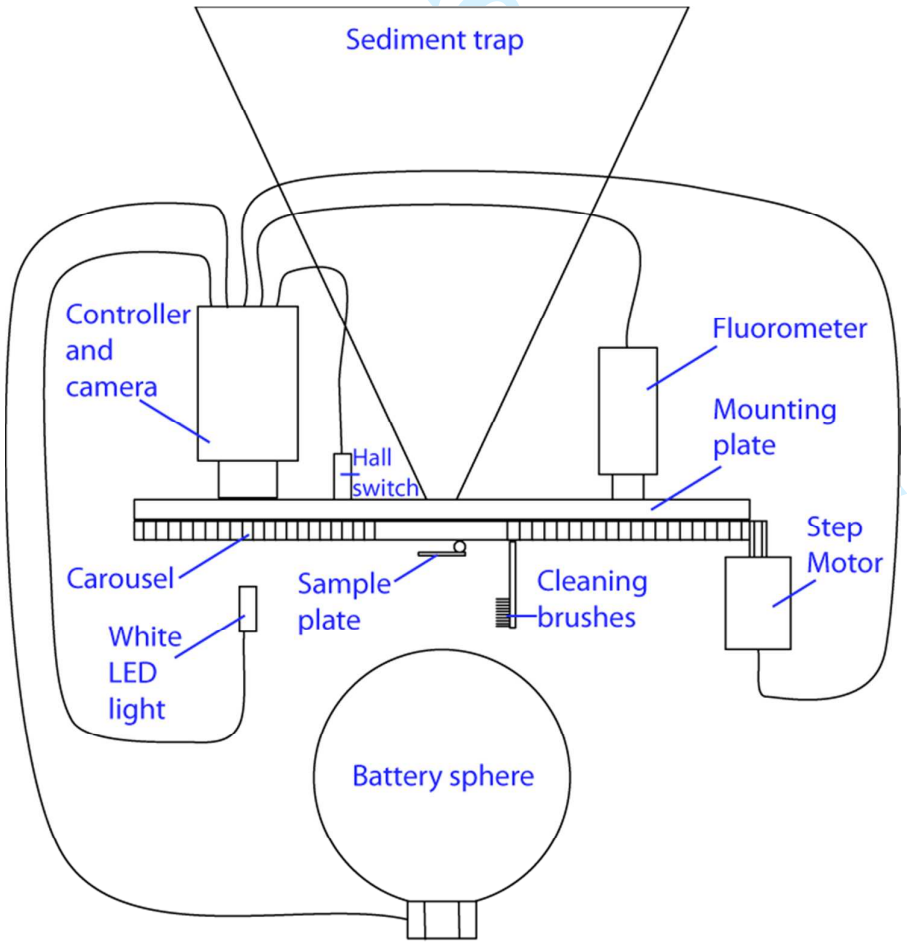

Figure 2. Placement of major system components. A funnel collects sinking particulate matter, which is then imaged and analyzed by a downward-looking camera and a fluorometer. A large battery, in a titanium sphere, powers the system for more than a year. Components not drawn to scale.

Figure 3. Carousel assembly viewed from below. Sample bottles have been replaced with a white, translucent sample collection plate, which is rotated through collection (1), fluorometry (2), and imaging (3) stations. A light-emitting diode (LED) light at the lower-left illuminates the sample from below for imaging. After the sample has been analyzed, it is discarded and the sample plate is passed through a set of cleaning brushes (4). The clean sample plate is then rotated back to the base of the funnel to begin collecting the next sample.

Alternatively, the carousel can be left in a flow-through position such that the sample plate is not beneath the base of the funnel, and the sinking particulate matter flows through a hole in the carousel plate without being collected. This allows the sample analysis interval to be longer than the collection time to avoid accumulating too much material on the sample plate during long analysis intervals or during times of heavy particulate flux. For example, a

sample can be collected for two hours, followed by a four-hour flow-through mode before collecting another two-hour sample.

Sensors and electronics

Most of the SES sensors and electronics are contained within three titanium pressure housings: two cylindrical housings hold the fluorometer and the camera + system controller, while a spherical case holds the large battery that powers the system (Fig. 2, 3). The original McLane sediment trap had a simple controller to advance the sample bottle carousel to each position at a programmed interval. A much more sophisticated controller is required to interface to the SES camera and fluorometer. The new controller uses a PC/104 board stack comprised of an ARM9-based CPU board, a relay board to switch power to the lights and sensors, and an RS-232 serial interface board to connect the sensors to the CPU. A separate stepper motor controller board (Allmotion model EZ-17) drives the original McLane carousel motor to move the sample plate between the collection, imaging, and fluorometry stations. A Hall-effect switch senses the position of the carousel to index the stations.

A 5-megapixel color digital camera (Allied Vision Technologies model GC2450C) equipped with 12-36 mm C-mount varifocal video lens (Computar model 11A) captures images of the particulate matter collected on the sample plate. The camera looks down on the sample through a flat-glass viewport. Each pixel in the image represents a distance of 13.9 µm on the 25-mm-diameter sample plate, yielding 72 pixels per mm.

The camera lens is not accessible for adjustment inside the sealed controller housing when the SES is deployed. Therefore the zoom, focus, and aperture of the lens were pre-adjusted on the bench, without the housing, using a test target positioned at the precise distance in air required to simulate the combined optical thickness of the glass viewport and water interface. This in-air distance was calculated from a computer-aided design model of

the assembly based on the thicknesses and refractive indices of the optical elements. While the "mechanical distance" of the glass and water between the camera lens and sample plate is 113 mm, the "optical distance" in air is only 82 mm. Once the focus was set, the aperture was adjusted to provide a depth of field of +1.6/-3.2 mm. The camera lens, adjusted using this procedure, required no further readjustments once the SES was submerged.

The sample plate is made of translucent white high-molecular-weight polyethylene to act as a volumetric light diffuser capable of operating underwater and at high ambient pressure. Its thickness is 10 mm, selected as a compromise between light uniformity across camera field of view and efficiency of light transmission. The 31.5 mm diameter of the plate was selected to be slightly larger than the 25 mm clear viewport aperture to allow for some inaccuracy in the mechanical indexing of the carousel.

Two LED lights illuminate the sample: a ring light surrounds the camera lens inside the housing and illuminates the sample from above, while an external light in its own pressure housing provides illumination through the bottom of the translucent sample plate (Fig. 3). The LEDs in both lights are T-1¾ Lumex SLX-LX5093UWC/C. The ring light uses eight LEDs positioned at 20 degrees relative to the lens centerline so the light beam of each LED crosses the centerline and illuminates the opposite side of the plate to eliminate shadows. The external light has a custom titanium pressure housing with an 8-mm-thick flat quartz window. The housing contains three LEDs equally spaced around the centerline with their light beams parallel to the centerline. To achieve a compromise between uniformity of illumination and efficiency of light delivery, the vertical position of the external LED light housing was first adjusted in air to achieve the desired image brightness and uniformity. Then the distance was increased by the ratio of the water-to-air refractive indices to correct for

166 underwater illumination. The final mechanical position of the light source is about 70 mm
167 under the sample plate.

168 The SES fluorometer was designed to detect the presence of chlorophyll *a* and
169 accessory pigments in the collected samples. This allows the instrument to distinguish
170 phytodetritus from other material. The fluorescence data are acquired by an optical two-band
171 fluorometer that analyzes sediment collected on the sample plate. Built at the Monterey Bay
172 Aquarium Research Institute, the fluorometer is sensitive in the 590×10 nm and 690×10 nm
173 optical bands, which approximate the centers of the chlorophyll *a* and phycoerythrin emission
174 bands respectively (Yentsch and Phinney, 1985). The fluorometer is installed in a separate
175 pressure housing connected to the controller housing with underwater cables for power and
176 data signals (Fig. 2). Fluorescence excitation is provided by a blue LED (Lumileds model
177 LXHL-NB98) followed by a 480×30 nm bandpass filter to minimize crosstalk between
178 optical channels.

179 The fluorescence detectors are comprised of two photomultiplier tubes (PMTs) each
180 integrated with a high-voltage power supply and interface electronics into a self-contained
181 module (Hamamatsu model H7155 for the 590 nm band, and H7155-01 for the 690 nm band)
182 operating in photon-counting mode. Each PMT has a set of neutral density filters installed in
183 light-tight enclosures along with 590×10 nm and 690×10 nm interference filters immediately
184 in front of each PMT to protect them from possible exposure to bright light. The light paths to
185 the two detectors and the excitation LED are combined by two generic dichroic 25 mm, 45˚
186 filters. The first one reflects blue light of wavelengths less than 510 nm from the LED 90˚ to
187 the sample plate and passes the resulting fluorescence signal to the detectors. The second
188 filter reflects yellow 550–620 nm light to the 590 nm detector, and transmits red light to the

690 nm detector. In addition, a 25 mm aluminum-coated first-surface mirror is used in front of the 590 nm channel PMT to fold the optical path, reducing the size of the fluorometer.

The fluorometer contains a microprocessor to control its functions and to communicate with the computer board stack in the main housing (Fig. 2). The integration time, i.e. the length of time that the excitation LED is on and the PMTs are measuring fluorescence, is programmable from 1 ms to 10 s in 1 ms steps. Measurements can also be made with the excitation LED off. If the particulate matter sample is not at the fluorometer position, this allows the measurement of the PMTs' dark current, which can be subtracted from the subsequent fluorescence measurement to improve accuracy. If the sample is at the fluorometer position, dark measurements can detect luminescence, or phosphorescence if the sample has just been illuminated by a fluorescence measurement.

Calibration of the SES fluorometer presents a challenge. Commercially available fluorometers measure chlorophyll in units of µg/l, and are presumed to operate in an infinite, homogeneous liquid medium. These fluorometers can be calibrated by placing them in solutions of known chlorophyll concentration. The SES fluorometer, however, measures fluorescence from solid targets of unknown size or distribution at a fixed distance. We could find no solid, calibrated chlorophyll *a* standard target and thus the assignment of metric units to the output cannot be justified. Therefore the output of the SES fluorometer is presented in photomultiplier counts per second based on measurements with a 1 s integration time. The count rates are interpreted relative to each other and represent the relative presence or absence of fluorescing material in the sample. To test whether an increase in the amount of fluorescent material yielded a linear increase in photomultiplier counts, we fabricated calibration disks containing linearly increasing areas of a dyed acrylic known to provide a stable fluorescence response at both 590 and 690 nm. Plexiglas Satinice® plum 4H01 DC

(polymethylmethacrylate) was chosen as the reference material because of its photostability and suitable combination of readings by a chlorophyll *a* sensor in another study (Earp et al., 2011). This material is 6 mm thick and was cut to rounds with target areas of 1.0, 2.0, 3.0 and 4.0 cm^2. Targets were placed in the center of the SES slide area. We compared the readings of this reference material to readings of the adaxial surface of a 3.2 cm^2 cutting of a fresh leaf.

Both the 590 nm and 690 nm fluorescence readings increased with increasing amount of fluorescent reference material on the slide (Fig. 4). For the 690 band:

$$\text{fluorescent reading}_{ref690} = 8.0 + 25 \times \text{target area}_{ref} \ (R^2 = 0.98).$$

Fluorescence readings in the 690 band consistently increased with target area for slide coverage up to 4 cm. For the 590 nm band, the linear relationship between fluorescence reading and target area was:

$$\text{fluorescence reading}_{ref590} = 33 + 13 \times \text{target area}_{ref} \ (R^2 = 0.84).$$

In the 590 band, an increase in area beyond 3 cm^2 did not contribute to additional photomultiplier counts, and background readings were variable when there was no reference material on the slide. We therefore recommend interpreting readings of the 590 band with caution when particle coverage is lower than 20% or exceeds 60 % of the slide. Compared to the reference material, readings of the leaf cutting were higher in the 690 band (400 ± 9.6 S.E. PM counts) and lower in the 590 band (10 ± 4.3 S.E. PM counts).

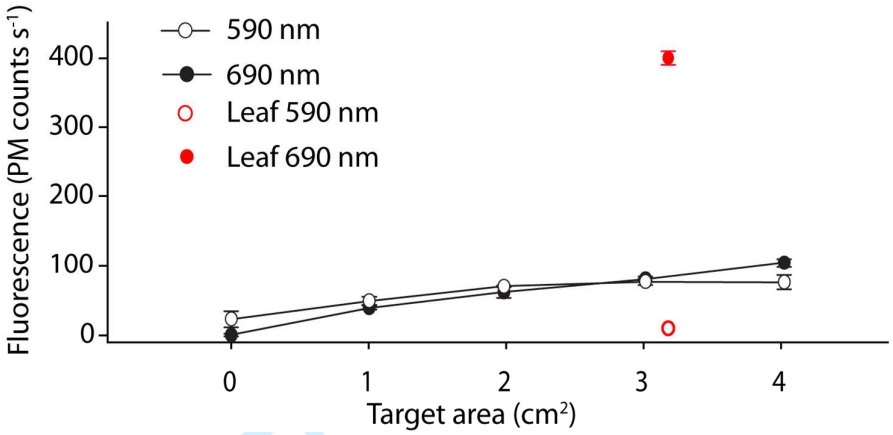

Figure 4. Fluorescence readings (average ± standard error) for reference targets [black; Plexiglas Satinice® plum 4H01 DC (polymethylmethacrylate)] and a leaf cutting (red) of varying size, based on a 1 s integration time. Open circles show readings at 590 nm, and dots show readings at 690 nm.

Two battery options are available to power the SES. A large 28 V battery comprised of 240 alkaline D cells powers the SES system. The battery provides about 2500 Wh of energy, which is enough to process more than 1500 sediment samples. A lithium primary battery has also been designed that can increase the energy capacity to almost 10 kWh to process more than 6,200 samples. The SES collects particulate matter for the vast majority of a deployment, so it is critical that all the electronics can be put into a very low-power state while the system is "sleeping" and collections are taking place, or the slide is in pass-though position. This goal is accomplished by a custom power controller board, which has DC-to-DC converters to convert the 28 V battery voltage to the 5 V and 12 V required by the system. The power controller is capable of providing up to 39 W while the system is processing a sample, although the current system uses less than 10 W. Once the sample is processed and the sample plate is back in the collection position, the power controller

removes power from the rest of the system and enters a sleeping state, consuming less than 1 mW until waking the system for the next sample analysis. This approach allows the use of commercial computer boards and sensors that are not optimized for low power consumption, while still keeping the average power consumption of the system low enough for year-long deployments.

Software

The design of the software system used in the SES was driven primarily by the requirement for unattended operations to abyssal depths with long service intervals of up to a year. The system requires reliable operation of the SES components, mission data management, and the capability to resume the mission after scheduled hibernation periods or unscheduled restarts. The resulting system design emphasizes simple, robust functionality over cutting-edge techniques with the objectives of predictable mission programming, minimal energy use, and easy servicing in the field.

Figure 5 is a high-level diagram of the software architecture. Generally, commands flow from the top of the diagram toward the bottom and information is filtered from bottom to the top. Higher-level logic is conducted as you move up in the diagram.

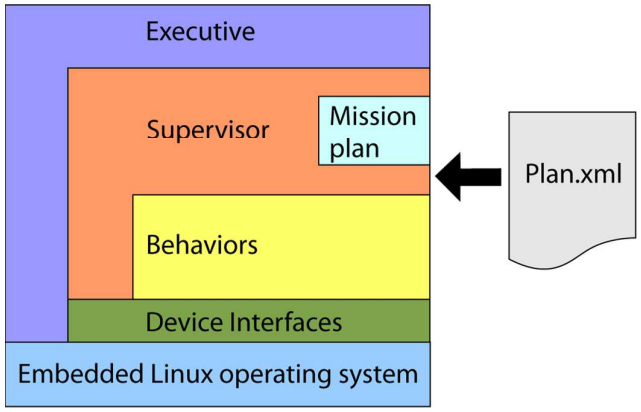

Figure 5. Diagram of the software architecture, consisting of Ruby and C application code running on a Linux operating system. The Mission Plan is read by the Supervisor, which executes the required Behaviors through the Linux Device Interfaces. The Executive monitors the Supervisor and communicates with the user during setup and recovery.

At the base is a stable and reliable Debian-based Linux kernel and operating system tailored for embedded systems. Communication with the sensor and actuator devices is handled using the conventional Linux serial and networking protocols, using both C and Ruby programming languages. The SES system design also relies on the simple and proven process management tools available in Linux to both automatically start the control system at boot time, and to restart the system should it fail unexpectedly.

Layered onto the operating system are the interfaces to the SES system components. The interfaces are designed to be used during short, focused dialogues, as the devices will usually be turned off between sessions. Any special handshaking required with a device is handled within the interface, providing a simple interface to higher-level functions. Low-bit-rate serial protocols are used to communicate with the carousel motor driver, power controller board, and fluorometer, while the imaging camera is controlled using the Ethernet driver provided by the camera manufacturer. The relay board used to switch power to the peripheral devices is controlled using shared memory on the computer bus.

The Behavior layer is where most of the SES control logic resides. Behaviors can be described best as functional units of operation that define what the instrument can be tasked to do. An example of a Behavior is `MoveCarousel`, which moves the carousel to a given position. In the SES control system Behaviors run one at a time, have complete control of the instrument during execution, and leave the instrument in a default state when completed. By

leaving the SES in a default state, a user is able to combine behaviors in arbitrary ways to produce unique mission plans.

A Mission Plan is the method by which a user defines the operation of the SES during a deployment. A typical mission might require the following Behaviors:

1) Rotate the carousel to the flow-through position so the funnel can fill with water upon SES deployment.
2) Sleep for 4 h while the SES sinks to the seafloor.
3) Rotate the carousel to the sample-collection position.
4) Sleep for 4 h while the sample is collected.
5) Rotate the carousel to the fluorometer position and make measurements.
6) Rotate the carousel to the camera position and capture images.
7) Rotate the carousel through the cleaning brushes to discard the sample and stop at the sample collection position.
8) Jump to step 4 to repeat the cycle until the mission is over.

These Behaviors are specified sequentially in a text file using a simple XML (Extensible Markup Language) format. Figure 6 is an example of a mission file. The first line contains the `Plan` element where the user specifies the number of iterations of the list using the sites attribute. Inside the `Plan` element the mission author simply lists the Behaviors to execute in the desired sequence. The names of the different Behavior types (e.g., `HomeClean`) hint at the function of each Behavior, but each can also be documented using the `name` and `comment` attributes. The other Behavior attributes relate to the task each type of Behavior performs, and are unique to each type. For example, the `location` attribute of the `MoveCarousel` Behavior relates to the position to which the carousel will move.

```
<Plan name="Observation Plan" sites="120" comment="About 3-hrs per site">

  <!-- Run nominal plan, take images, log flourometer data, rinse & repeat -->

  <HomeClean comment="Pass through cleaning station on my way home" />

  <MoveCarousel name="To Collection Pos" location="collection" />

  <Pause name="3 hour collection"  hibernate_for="180" delay_for="0.5" />

  <MeasureFluorometry name="Ref Fluorometry" dark_time="1000" ref_time="1000" />

  <MoveCarousel name="To Fluorometry Pos" location="fluoro" />

  <MeasureFluorometry lum_time="1000" flu_time="1000" phos_time="1000" />

  <MoveCarousel name="To Camera Pos" location="camera" />

  <FluoroImage prefix="pulse61_" />

</Plan>
```

Figure 6. Segment of a mission plan, consisting of a list of behaviors specified sequentially in a text file using a simple XML format. In this case with XML, tags are navy, attribute names are green, attribute values are light brown, and comments are grey.

The Supervisor is responsible for managing the execution of the Mission Plan. At the start of the process the plan file is loaded and parsed, resulting in a Behavior list. The Supervisor steps through the list executing each Behavior one at a time, repeating the list based on the number of sites specified in the plan file. The Supervisor also manages restarts after hibernation periods during which the instrument draws very little power. When hibernation is requested by a Behavior, the Supervisor saves the state of the instrument to a small execution database. The saved state is loaded after the Mission Plan on restarts and the Supervisor resumes mission execution from where it left off.

At the top of the architecture is the Executive. The Executive is started automatically by the Linux system during the start-up process and is responsible for launching the Supervisor and responding to external messages. The Executive launches the Supervisor in such a way that, should the Supervisor process unexpectedly quit due to an unhandled exception, the Executive will receive a signal from the operating system and the Supervisor

will be restarted. External messages come from the system console and request system information such as the current behavior and battery voltage, or command an action from the instrument. Commands include stopping the current Mission Plan, loading a different Mission Plan, and requesting the system to reboot.

Mission science data are stored on a 32 GB Compact Flash memory card. Camera images are stored in their native Bayer-16 format, and are converted to TIFF images by a batch process after the SES has been recovered. This reduces data storage requirements, as the Bayer-16 images are about one-third the size of the TIFF images (10 MB versus 30 MB), and it conserves the battery energy that would be required to convert the images in situ. The vast majority of data storage is taken up by camera images, with the remainder used for fluorometer readings and engineering data such as battery voltage. The software also maintains extensive log files to record every action taken by the SES in order to verify correct operation and to help determine the cause of any malfunction.

Assessment

Testing

The SES was first tested in the 1.5 million liter, 10 m deep saltwater tank at the Monterey Bay Aquarium Research Institute to verify basic functionality. This also enabled adjustment of the LED light intensities for optimal camera exposure in water.

After tank testing, the SES was deployed on the MARS (Monterey Accelerated Research System) cabled observatory in Monterey Bay, 37 km from shore at a depth of 900 m (Henthorn et al. 2010). Cable interface electronics were installed in the SES battery housing to allow the instrument to receive power and data connections from the MARS network, permitting shore-based researchers to control the SES and receive images in real time. This capability proved to be invaluable as repeated cycling revealed an infrequent but

serious flaw in the sample plate cleaning mechanism, causing the carousel to jam in a way that could not be corrected without recovery of the instrument. The SES was recovered and redeployed two more times on MARS before modifications to the sample mechanism were deemed reliable enough for autonomous deployment at greater depths offshore.

Station M deployments

In June 2012, the SES was deployed at Station M (34° 50' N, 123° 00' W), a long-term study site located 220 km offshore of the central California coast (Smith et al. 2013). A mooring held the SES at a depth of 3910 m, 50 m above the seafloor at 3960 m. This site has been the focus of a long time-series monitoring program since 1989. Other instruments at the study site include a wide-area seafloor time-lapse camera, a benthic rover vehicle, and traditional sediment traps.

For the first Station M deployment the SES was programmed to process a sample every 12 h. When the instrument was recovered in November 2012, it had processed a total of 304 samples, the expected number for the five-month deployment. Initial inspection of the images revealed times when the sample plate was completely covered with sediment, resulting in some images being almost completely dark. Because fully dark images obscured image interpretation, the sample interval was reduced to 3 h for the second deployment in November 2012, aiming to collect less material per image. When the instrument was serviced after another seven months in June 2013, it had processed an additional 1,200 samples, stopping as programmed before the battery was depleted.

The third SES deployment was the longest, lasting ten months from June 2013 until April 2014. The SES recorded a total of 1,420 samples processed at 4 h intervals, stopping only when the flash memory card filled. For the first two deployments, the collection time was equal to the sample interval (12 and 3 h respectively). However, the collection time was

reduced to only half the sample interval for the third deployment (2 h collect, 2 h standby) with the carousel in a flow-through position that collects no sediment for the remainder of each sample interval. These results are summarized in Table 1.

Table 1. Samples processed on first three deployments of Sedimentation Event Sensor

Deploy number	Duration	Sample interval	Collection time	Samples processed
1	5 mo	12 h	12 h	304
2	7 mo	3 h	3 h	1,200
3	10 mo	4 h	2 h	1,420

Results

Images

The macro photographs revealed detail about the size distribution and composition of collected sediments. Figure 7 shows typical images. Most of the material on the sample plate consisted of aggregations of phytodetritus along with fecal pellets of various types and sizes. Sometimes a whole animal was collected, such as the small crustacean seen in panels 6a and 6b. The backlight provided the best illumination for interpreting most of the images. For instance, the gut of the crustacean is clearly visible in panel 6b. However large, opaque objects such as the salp fecal pellet in panel 6c were best viewed with front lighting, as seen in panel 6d. Note the blue cast to the light in the front-lit image. Both the front and back lights use the same type of white LED, but the backlight passes through much more seawater, filtering out the shorter wavelengths.

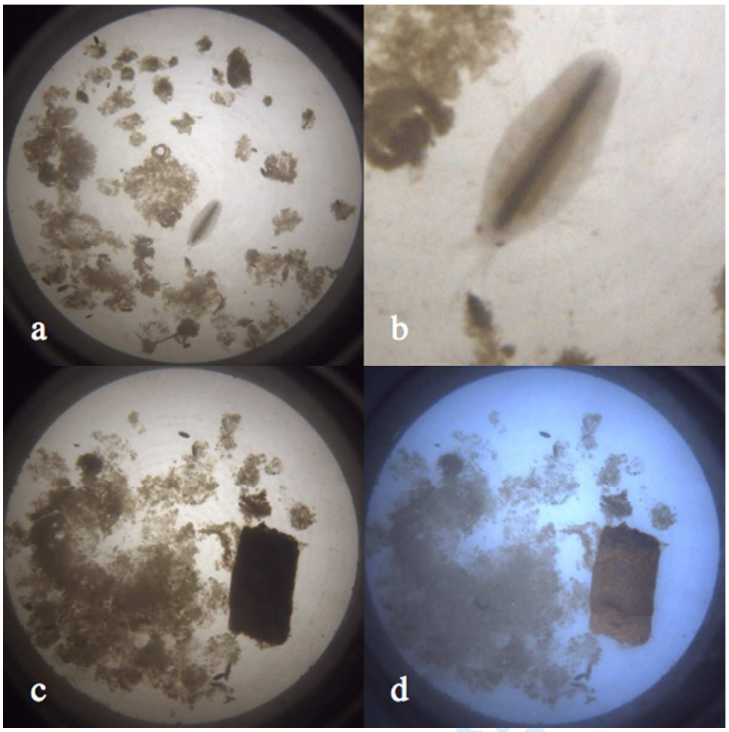

Figure 7. Sample images from SES deployment at Station M: a) Typical sample with a variety of organic material on the 25 mm diameter sample plate; b) Detail of sample in panel (a) showing a small crustacean about 3.9 mm long with legs and gut visible; c) Back-lit image with a large rectangular salp fecal pellet; d) Front-lit image of sample shown in panel c, showing more detail of the same salp fecal pellet.

Although a detailed analysis of each SES image can be made, it is also possible to make simpler measurements in order to get a broad perspective of sedimentation rates during a deployment. Figure 8 shows the mean pixel brightness of each image recorded between June and November of 2012. The brightness values were scaled so that a completely empty sample plate, resulting in the brightest image, represents a light attenuation factor of 0%. A sample plate completely covered with material reaches about 95% attenuation as a small amount of light still leaks through the sample. From this measurement we can see that sedimentation rates were quite high at the beginning of the deployment, then diminishing

418 through June, July, and the first half of August 2012. In the last week of August, a pulse of
419 material was detected with a sudden onset and conclusion, lasting about ten days. This pulse
420 of material was followed by highly variable sedimentation rates from mid-September to mid-
421 October. Almost no material was collected during the third week of October, and then
422 episodic pulses of material were seen until the end of the deployment in the first week of
423 November.

424

425

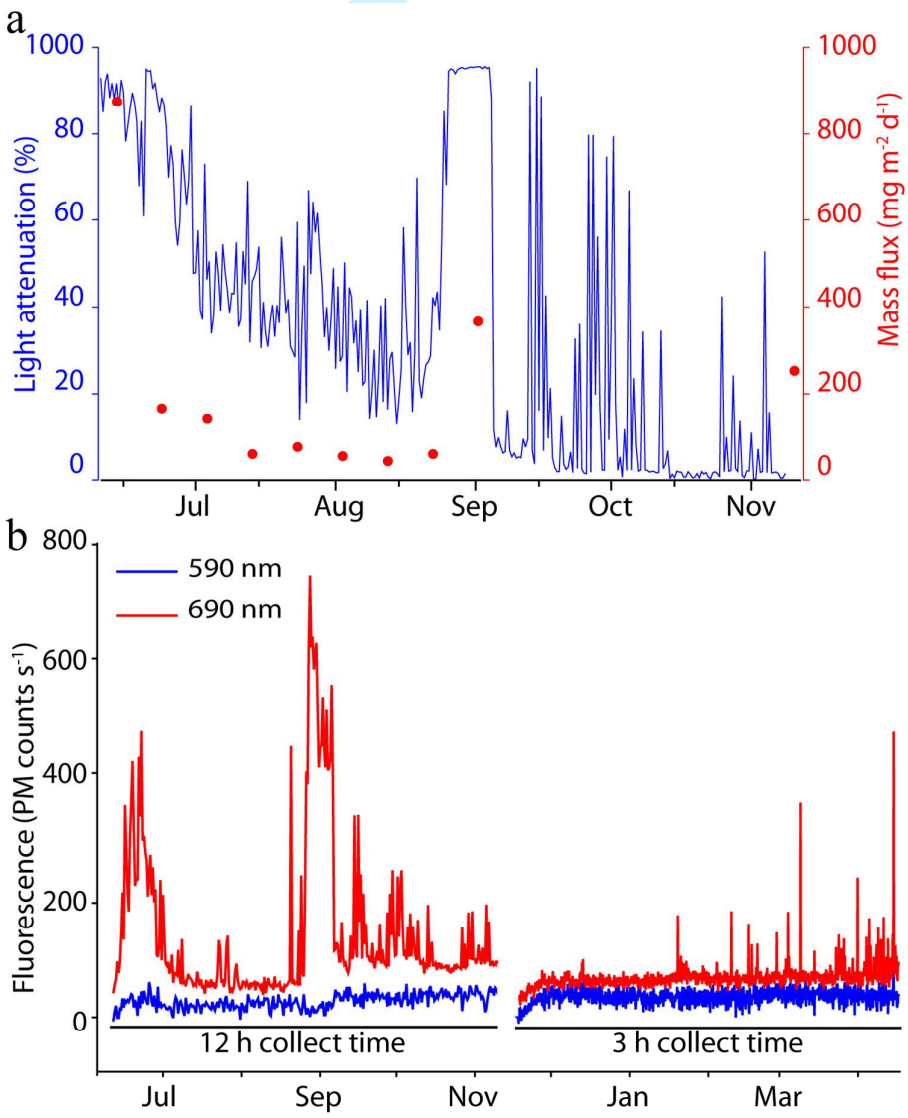

426

Figure 8. SES data collected at Station M in 2012. a) Relative sediment quantity collected by the SES determined by measuring the mean brightness of the sample plate images (blue line and axis) based on integrated transmissometer readings. Sedimentation rates determined by the SES were comparable to mass flux measured by concurrently deployed sediment traps at the same station and depth (red axis, with each dot representing the average value for the previous ten day collection period). a) Fluorometer readings during two consecutive deployments with different collect times. The vertical axis values are photomultiplier counts per second. Sustained periods of material fluorescent in the 690 nm band (chlorophyll *a*) were seen during the first deployment, but not during the second deployment.

Sedimentation rates as determined by the SES were compared to those from a traditional sediment trap operating at Station M during the same period. Both sampling methods were moored 50 m above bottom, but kilometers apart. Sample bottles from the traditional trap, which collected at ten-day intervals, were returned to the lab, freeze-dried, and then weighed to determine the total dry mass of collected material. Mass flux (mg m^{-2} d^{-1}) was calculated using this measure, divided by the baffle opening size and the collection time. Each red dot in Fig. 8a represents the average quantity of sediment collected daily during the previous ten-day period. No mass flux data are available for the months of September or October 2012 due to a clog in the traditional sediment traps, and the last data point shows the sudden release of a large quantity of sediment after the clog cleared. Clogging and subsequent clearing are recurring problems with traditional sample collection that the SES is intended to, and did, ameliorate. For the times when both instruments collected material contemporaneously, the same general trends in sedimentation rates were seen. There were differences, but this is to be expected because they differed in exact location

and collect time. Additionally light attenuation is a non-linear proxy for material mass. because the collected sediment piles on top of itself, adding mass presumably without a linearly corresponding increase in the amount of light blocked.

Fluorometry

We analyzed fluorometer data collected using a 1 s integration time. Figure 8a shows the fluorometer record from the first two deployments, spanning a time period of 11 months. The collection time of material through the funnel was 12 h for the first deployment and 3 h for the second deployment, so y-axis values cannot be directly compared between the two deployments for scientific interpretation. General features of activity during the period, however, can be observed.

The gap in November between the two deployments is the time that the SES was on the ship being serviced. The first week of each deployment showed a slow change in fluorescence, starting at zero and increasing over a period of about a week to more typical levels. Examination of the first week of images from each deployment revealed condensation on the optical viewports of the instrument housings, despite the use of desiccant and dry-nitrogen purging of the housings. Deployment procedures have since been modified to increase both the quantity of desiccant and the time of the dry-nitrogen purging in order to rectify this problem.

Two pulses of material possibly bearing chlorophyll *a* can be seen on the 690 nm record in June, and again from late August to early September of 2012. These times corresponded to the periods of the highest sedimentation rates seen in Fig. 8a, as well as record-high depositions of salp fecal-pellets and phytodetritus on the sea floor at Station M as detected by a benthic rover (Smith et al. 2014). Note however that during July and August, when sedimentation rates were still quite high, fluorescence was low. This result implies that

material collected during those times had a fundamentally different composition than that collected during the other pulse events. The second deployment showed no sustained pulses of fluorescent material, however extremely brief pulses, comprising a single sample each, were seen. No significant activity was evident on the 590 nm record for either deployment.

Discussion

The SES has proven to be a reliable instrument, processing 2,924 samples on its first three deployments with no malfunctions. This reliability was achieved through rigorous testing on the MARS cabled observatory at 900 m depth before long-term deployment in deeper water. Design and construction of the SES was greatly facilitated by basing it upon a proven commercial sediment trap. Custom power control circuitry allows the system electronics to be built from inexpensive commercial microcontroller boards and peripherals, and greatly shortened the hardware development time. The use of the open-source Linux operating system and Ruby programming language also help to lower system costs.

Initial examination of the data from these deployments has revealed that both the deposition rate and composition of settling particulate matter at Station M is highly variable on time scales as short as a few hours. While the SES does provide high-resolution images of the collected samples, it does not retain those samples and thus cannot provide direct measures of mass flux or further analysis of carbon content. Flux values generated from the SES will need to be estimated from models based on concurrent sediment trap and SES sampling periods. However, the SES can measure the fluorescence of the samples in situ, where this information is lost in the stored samples of a traditional sediment trap (Vaulot et al. 1989). Phytodetritus is a high-quality food source for deep-sea communities (Fitzgeorge-Balfour et al. 2010), so the ability to estimate the chlorophyll content of settling material has

498 strong scientific value. Given these functional differences, the SES is best used to
499 complement rather than replace traditional sediment traps.

500 The Carbon Flux Explorer was first deployed in 2007 to measure aspects of sinking
501 particulate matter content while avoiding the necessity of sample retrieval. It increases both
502 deployment duration and sampling frequency beyond that of traditional sediment traps, but
503 differs from the SES in its deployment modes. The Carbon Flux Explorer integrates an
504 Optical Sedimentation Recorder with a Sounding Oceanographic Lagrangian Observer float
505 to estimate both particulate organic carbon and particulate inorganic carbon fluxes in the
506 upper 1000 m of the water column (Bishop 2009). Its Optical Sedimentation Recorder uses a
507 camera with multiple light sources to image particles collected on a horizontal optical
508 window. After the images are analyzed in-situ, the particulate organic and inorganic carbon
509 estimates, image thumbnails, and engineering data are sent to shore via satellite. This
510 vertically profiling float is autonomous and Lagrangian, capable of analyzing samples every
511 half hour for one to two months. While suitable for drift studies with large geographic
512 coverage, the Carbon Flux Explorer is less appropriate for prolonged studies at a single
513 station, and at abyssal sites. Table 2 outlines the respective capabilities of the Carbon Flux
514 Explorer and the SES.

515 Future work with the SES includes adding battery capacity and memory storage to
516 increase the deployment time beyond a year, further reducing the use of expensive ship time
517 spent servicing the instrument. A shorter and simpler version of the SES frame, eliminating
518 the drop-weight mechanism, would allow the instrument to be deployed anywhere along a
519 mooring string, from midwater to shallow depths. The SES software permits the sampling
520 interval and collection time to be varied easily, although the optimum settings will depend
521 upon location and season. Enhanced instrument software could set the collection time

522 dynamically during the deployment based upon a density analysis of the previous sample
523 image, although material collected with non-uniform collection times would be more difficult
524 to analyze quantitatively. The current platform invites the development of additional sensors,
525 such as an imaging fluorometer to reveal more detail about the composition of collected
526 samples.
527
528 Table 2. Comparison of Sedimentation Event Sensor and Carbon-Flux Explorer (Bishop
529 2009).

	Sedimentation Event Sensor	Carbon Flux Explorer
Deployment Method	Moored	Free-drifting
Sample Illumination	Front, back	Front, side, cross-polarized
Fluorometry	Yes	No
Samples per Deployment	6,200	~2000
Real-Time Data Recovery	No	Yes
Full-Resolution Images Recovered	Yes	No

530
531
532
533
534

References

Bishop, J. K. B. 2009. Autonomous observations of the ocean biological carbon pump. Lawrence Berkeley National Laboratory.

Buesseler, K. O., A. N. Antia, M. Chen, and others 2007. An assessment of the use of sediment traps for estimating upper ocean particle fluxes. J. Mar. Res. 65: 345.

Earp, A., C. E. Hanson, P. J. Ralph, and others 2011. Review of fluorescent standards for calibration of in situ fluorometers: Recommendations applied in coastal and ocean observing programs. Optics Express, 19: 26768-26782.

Fitzgeorge-Balfour, T., D. S. M. Billett, G. A. Wolff, A. Thompson, and P. A. Tyler. 2010. Phytopigments as biomarkers of selectivity in abyssal holothurians; interspecific differences in response to a changing food supply. Deep-Sea Res. II. 57: 1418-1428.

Henthorn, R. G., B. W. Hobson, P. R. Mcgill, A. D. Sherman, and K. L. Smith. 2010. Mars benthic rover: In-situ rapid proto-testing on the monterey accelerated research system. 1-7. IEEE.

Honjo, S. 1980. Material fluxes and modes of sedimentation in the mesopelagic and bathypelagic zones. J. Mar. Res. 38: 53-97.

Honjo, S., and K. W. Doherty. 1988. Large aperture time-series sediment traps; design objectives, construction and application. Deep-Sea Res. A. 35: 133-149.

Knauer, G. A., J. H. Martin, and K. W. Bruland. 1979. Fluxes of particulate carbon, nitrogen, and phosphorus in the upper water column of the northeast Pacific. Deep-Sea Res. A. 26: 97-108.

Smith, K. L., H. A. Ruhl, M. Kahru, C. L. Huffard, and A. D. Sherman. 2013. Deep ocean communities impacted by changing climate over 24 y in the abyssal northeast Pacific Ocean. Proc. Nat. Acad. Sci. 110: 19838-19841.

559 Smith Jr, K. L., A. D. Sherman, C. L. Huffard, P. R. McGill, R. Henthorn, S. Von Thun, H.
560 A. Ruhl, M. Kahru, and M. D. Ohman. 2014 Large salp bloom export from the upper
561 ocean and benthic community response in the abyssal northeast Pacific: Day to week
562 resolution. Limnol. Oceanogr. 59: 745-757.
563 Vaulot, D., C. Courties, and F. Partensky. 1989. A simple method to preserve oceanic
564 phytoplankton for flow cytometric analyses. Cytometry 10: 629-635.
565 Yentsch, C. S., and D. A. Phinney. 1989. Spectral fluorescence: an ataxonomic tool for
566 studying the structure of phytoplankton populations. J. Plankton Res. 7: 617-632.
567
568

Acknowledgments

The authors wish to thank Rob Glatts and Fred Uhlman for their work on an earlier version of the SES at the Scripps Institute of Oceanography. Funding was provided by the David and Lucile Packard Foundation.